Astron. Astrophys. 325, 414–424 (1997)

ASTRONOMY
AND
ASTROPHYSICS

Direct neutron captures and the r-process nucleosynthesis

S. Goriely

Institut d'Astronomie et d'Astrophysique, C.P. 226, Université Libre de Bruxelles, bd. du Triomphe, B-1050 Brussels, Belgium

Received 9 December 1996 / Accepted 18 March 1997

Abstract. The radiative direct capture of neutrons is calculated within the potential model. The uncertainties related to the choice of the neutron-nucleus interaction potential and the prediction of the excitation spectrum in the residual nucleus are discussed. The allowed direct $E1$-type transitions to all the excited states predicted by a combinatorial model of nuclear level densities are calculated with the introduction of an average spectroscopic factor. The resulting direct contribution to the neutron capture rate is estimated for all the neutron-rich nuclei potentially involved in the r-process nucleosynthesis and compared with the statistical compound nucleus contribution. The total radiative capture cross section is approximated and used in parametric r-process calculations to study the impact of the direct capture mechanism on the r-process nucleosynthesis.

Key words: nuclear reactions; nucleosynthesis; abundances – stars: supernovae

1. Introduction

The rapid neutron-capture process, or r-process, is one of the main mechanisms able to explain the synthesis of the stable nuclides heavier than iron observed in nature. The r-process is believed to take place in environments characterized by high neutron densities ($N_n \gtrsim 10^{20}$ cm^{-3}), such that successive neutron captures can proceed into neutron-rich regions well off the β-stability valley. This process produces nuclei with decreasing neutron binding energies, and consequently faster (γ, n) photodisintegration, which at high temperatures ($T \gtrsim 10^9$ K) are able to compete with the slowing-down (n, γ) reactions. With timescales usually thought to be much longer than the characteristic timescale of the (n, γ) and (γ, n) reactions, the β-decays finally drive material to higher Z elements. To calculate the changes in abundance of the heavy nuclei as a result of these high neutron fluxes and high temperatures, a nuclear reaction network including all neutron captures, photodisintegrations, β-decays, as well as β-delayed processes, fission processes and α-decays must be used. Because of the formidable task to solve such a problem and to determine the neutron capture and photodisintegration rates for some 3000 (mostly unknown) neutron-rich nuclei, simplifying assumptions are usually made. The simplest and most widely used form of the r-process, commonly referred to as the canonical model, assumes that the neutron density and temperature not only remain constant over the whole time scale τ_{irr} of the neutron irradiation, but also that they are high enough, so that strong and electromagnetic interactions can occur on a much shorter time scale than the weak interactions. Under such conditions, an $(n, \gamma) - (\gamma, n)$ equilibrium can be reached for each isotopic chain, before any β-decay can take place. This assumption, also known as the waiting point approximation (WPA), has the major numerical advantage of replacing a set of about 3000 coupled differential equations by a system of about 80 simple equations, describing the abundance flow from one isotopic chain to the next. Moreover, the abundance ratio of 2 isotopes can now be expressed by the well known Saha equation depending on the temperature, partition functions and the neutron separation energies only (Seeger et al., 1965). Therefore, the WPA present the considerable advantage of being independent of the uncertainties related to the determination of the neutron capture and photodisintegration rates. Nevertheless, the validity of the WPA is a very subtle issue. In order to assess the consistency of the approximation made, a reliable estimate of these neutron capture and photodisintegration rates is mandatory. For this reason, the validity of the WPA has recently been studied (Goriely and Arnould, 1996). However, such an analysis still remains highly affected by the uncertainties related to the nuclear physics considered, and in particular to a reliable prediction of the (n, γ) rates.

So far, all the r-process calculations have made use of neutron capture rates evaluated within the statistical model of Hauser-Feshbach (Thielemann, et al., 1986). Such a model makes the fundamental assumption that the capture process takes place with the intermediary formation of a compound nucleus (CN) in thermodynamic equilibrium. The energy of the incident particle is then shared more or less uniformly by all the nucleons before releasing the energy by particle emission or γ-de-excitation. The formation of a compound nucleus is usually justified by assuming that the level density in the compound nucleus at the projectile incident energy is large enough to ensure an average statistical continuum superposition of available

Send offprint requests to: S. Goriely

resonances (e.g. Satchler, 1980). However, when the number of available states in the compound system is relatively small, the validity of the Hauser-Feshbach predictions has to be questioned, the neutron capture process being possibly dominated by direct electromagnetic transitions to a bound final state rather than through a compound nucleus intermediary. Direct reactions are known to play an important role for light or closed shell systems for which no resonant states are available (Mengoni et al., 1995; Beer et al., 1996). It has also been shown through a simple analytical model (Mathews et al. 1983) that the direct capture (DC) contribution may dominate the statistical contribution for heavy neutron-magic targets with low enough neutron binding energy. The direct neutron capture rates have unfortunately never been estimated for exotic neutron-rich nuclei as those produced by the r-process. Thus, the relative importance of the direct mechanism with respect to the statistical contribution remains cumbersome.

The present work aims at estimating in a microscopic model the influence of the direct neutron captures on the r-process nucleosynthesis. For this purpose, the potential model of direct captures is used, as described in Sect. 2. Emphasis is put on the uncertainties related to the determination of the neutron-nucleus interaction potential, and the excitation spectrum of the residual nucleus. In particular, our choice to estimate such a spectrum with a combinatorial model of nuclear level densities is discussed. The direct neutron capture cross section of all the nuclei potentially involved in the r-process nucleosynthesis is calculated in Sect. 3, and compared with the CN contribution obtained with the popular Hauser-Feshbach model. The total (n,γ) rate is then approximated taking into account the possible overestimate of the CN model predictions for neutron-rich nuclei. Finally, in Sect. 4, r-process calculations are performed in the framework of the single- and multi-event model and the influence of the newly-derived (n,γ) rates on the r-process abundance distribution is analyzed in detail.

2. The potential model of the direct radiative capture of neutrons

Many works on neutron capture reactions (e.g. Lane and Lynn, 1960; Lynn, 1968; Satchler, 1983) have been devoted to the description of the DC mechanism, in which the incoming neutron is scattered directly into a final bound state without forming a compound nucleus. In a general way, the total DC cross section of a nucleus (Z,N) can be expressed as

$$\sigma^{DC}(E) = \sum_f C_f^2 \; S_f \; \sigma_f^{DC}(E) \; , \tag{1}$$

where E is the energy of the incident neutron and the sum runs over all the available final states f of the residual nucleus. C_f is the isospin Clebsh-Gordan coefficient and S_f the spectroscopic factor, describing the overlap between the antisymmetrized wave function of the initial system $(Z,N)+n$ and the final state f in $(Z,N+1)$. Eq. 1 emphasizes the importance of the single-particle configuration of the final state (for which $S_f \simeq 1$) in the direct transition, other configurations leading to a negligible spectroscopic factor. The DC cross section σ_f^{DC} for the emission of electric dipole radiation (we will restrict ourself to the major $E1$ transition, as explained below) to the final state f is obtained (Christy and Duck, 1961; Baye and Descouvemont, 1985) from

$$\sigma_f^{DC}(E) = \frac{16\pi}{9\hbar} \; k_\gamma^3 \; \bar{e}^2 \; \mid Q_{i\rightarrow f}^{E1}(E) \mid^2 \; , \tag{2}$$

where $k_\gamma = \epsilon_\gamma/\hbar c$ is the wave number of the emitted γ-ray (of energy ϵ_γ) and $\bar{e} = -eZ/A$ is the $E1$ effective charge for neutrons. The matrix element, corresponding to the overlap of the initial scattering wave function in the entrance channel Ψ_i, the bound-state wave function Ψ_f and the electric dipole operator T^{E1}, is given by

$$Q_{i\rightarrow f}^{E1}(E) = \langle \Psi_f \mid T^{E1} \mid \Psi_i(E) \rangle = A_{l_i l_f} \; \mathcal{I}_{l_i l_f}(E) \; . \tag{3}$$

$A_{l_i l_f}$ corresponds to the angular part depending on the initial (l_i) and final (l_f) angular momentum of the transition and its expression can be found, for example, in Christy and Duck (1961). $\mathcal{I}_{l_i l_f}$ is the radial overlap that can be expressed as a function of the radial part of the entrance unit-flux scattering wave function $w_{l_i}(r,E)$ and of the final-state wave function $u_{l_f}(r)$:

$$\mathcal{I}_{l_i l_f}(E) = \int_0^\infty u_{l_f}(r) \; r \; w_{l_i}(r,E) \; dr. \tag{4}$$

The initial and final wave functions are determined within the potential model by solving the respective Schrödinger equations, in which the same analytical form of the potential is used for both channels. In particular, the depth of the potential is scaled in order to reproduce, in the final system the exact binding energy of the state f, and in the initial system the so-called volume integral per nucleon (if known) defined by

$$\frac{J_V(E)}{A} = -\frac{1}{A} \int V(\mathbf{r},E) d^3\mathbf{r} \; , \tag{5}$$

where A is the atomic mass and V the potential in the entrance channel. Different types of potential have been constructed, all of them presenting their own features. As it is classically assumed, we will neglect in the present study the imaginary part of the potential, which is thought to give a negligible contribution to the total cross section for nuclei with low neutron separation energy, because of the small flux into reaction channels. The DC mechanism is essentially a peripheral interaction taking place on the nuclear surface. Different potentials are usually characterized by different radii and diffusenesses, and are, therefore, expected to lead to different predictions of the DC cross section, especially for incoming s-wave neutrons[1].

To estimate the sensitivity of σ^{DC} to the choice of the interaction potential, we consider here 4 different potentials, namely a Woods-Saxon (WS) potential (Wilmore and Hodgson, 1964), the real part of the optical potential (OP) of Jeukenne et

[1] In the case of incident p-wave neutrons, Mengoni et al. (1995) showed that the DC cross section was relatively insensitive to the neutron-nucleus potential.

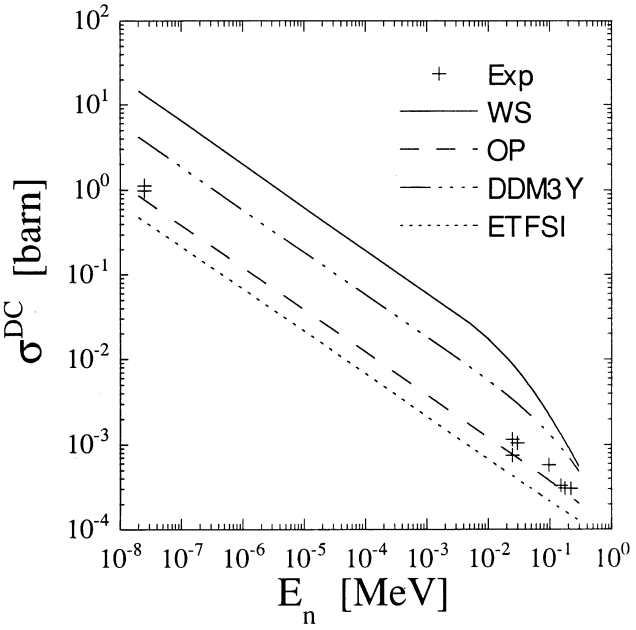

Fig. 1. Comparison of the experimental (crosses) neutron capture cross section on ^{48}Ca with the DC predictions obtained with the 4 different potentials, as described in the text.

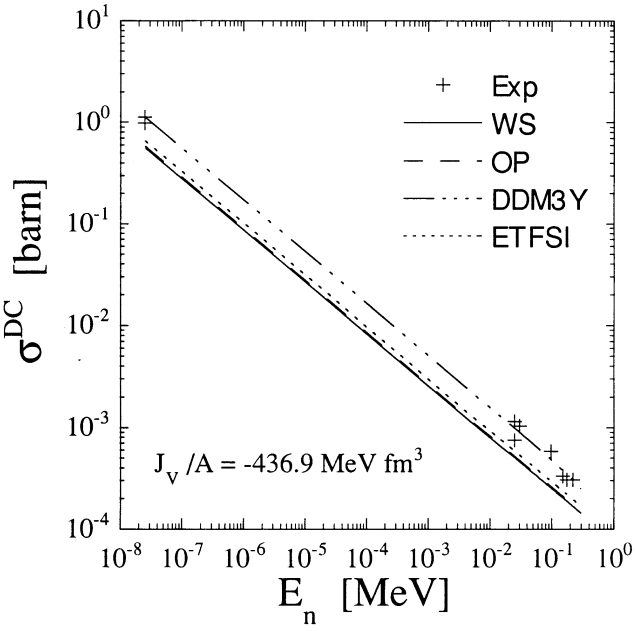

Fig. 2. Same as Fig. 1, when all the potentials in the entrance channel are scaled to reproduce the volume integral $J_V/A = -436.9$MeVfm^3

al. (1977), the ground-state single-particle potential of the Extended Thomas-Fermi plus Strutinsky Integral (ETFSI) model of Aboussir et al. (1995) and a folding potential with the density-dependent DDM3Y nucleon-nucleon interaction (Kobos et al., 1984). The radiative DC cross section of ^{48}Ca$(n,\gamma)^{49}$Ca has been calculated using the 4 above-mentioned potentials and all the experimentally available data, such as the the energy, spin, parity and spectroscopic factor of each excited state of ^{49}Ca (Uozumi et al., 1994). The influence of the potential form on σ^{DC} can be observed in Fig. 1, where no prior renormalization of the potential depth of the initial system is performed. As a consequence, they all predict different values of the volume integral, namely J_V/A[MeVfm^3] = $-508, -452, -422, -463$ for WS, OP, ETFSI and DDM3Y, respectively, and large deviations among them (reaching a factor of 30) can be seen. In contrast, in Fig. 2, the same potentials are used, but renormalized in such a way that they all fit the volume integral deduced from the experimental scattering length data, i.e $J_V/A = -436.9$MeV fm^3 (Krausmann et al., 1996)[2]. In this case, deviations within a factor of 2 are obtained when using the different potentials. This result reflects the well-known rule that cross sections calculated from various potentials are rather insensitive to their detailed form provided that they all have the same volume integral per nucleon.

However, when dealing with exotic nuclei as those involved in the r-process nucleosynthesis, no experimental data concerning the volume integral are available, and the use of a potential with arbitrary strength in the entrance channel could have an important impact on the DC cross section. Although little potentials are constructed in order to lead to good predictions of the volume integral, this requirement has been carefully kept in mind by Jeukenne et al. (1977) who determined their OP in order to reproduce the experimental volume integrals and root mean square radii in a wide range of the periodic table. For this reason, if no prior renormalization is performed (Fig. 1), the OP clearly gives the best agreement with the experimental data with respect to the other potentials considered. In addition, the OP of Jeukenne et al. (1977) is also a popular choice made in most of the Hauser-Feshbach calculations of radiative capture cross sections of neutrons, especially for nuclear astrophysics applications. Assuming that both CN and DC mechanism contribute to the neutron capture, only a coherent treatment of both parts could ensure a reliable prediction of the total (n,γ) cross section. This implies, of course, the consideration of the same interaction potential. Another interesting choice would be the ETFSI potential. As a matter of fact, the ETFSI model is based on a realistic potential derived from a Skyrme-type effective interaction which has shown its ability to reproduce other nuclear properties, such as the nuclear masses. For this reason, the ETFSI might be well suited to the estimate of the volume integral at low energies (although it is independent of the incident neutron energy), and more obviously of the final wave functions. Nevertheless, we will restrict ourselves to the use of the OP of Jeukenne et al. (1977) for the reasons mentioned above. It should be noted that the same potential is used for the description of the initial and final systems. In particular, the final potential is deduced from the OP prescription at zero energy (the scaling factor introduced to fit the binding energy of the final states is limited to a maximum ratio of 1.3, so that no exaggerate normalization

[2] Note that the so-called experimental volume integral has been derived making use of the DDM3Y potential, which therefore shows a better agreement with experimental cross sections.

of the OP depth is considered). Finally, forbidden transitions to already occupied states in the final nucleus are avoided by considering the single-particle configuration predicted by the ETFSI model.

A second important aspect in the calculation of the DC cross-section concerns the determination of the excited spectrum of the final system, as shown by Eq. 1. Such a prediction represents without doubt the most critical part of the calculation when dealing with experimentally unknown nuclei. It is well accepted that the predictions of the DC potential model are in qualitatively good agreement with experimental results as long as all the details of the excitation spectrum (energy, spin, parity and spectroscopic factor) are known experimentally, as seen in Fig. 2[3]. However, when dealing with nuclei for which a complete set of experimental data (especially regarding the characteristics of the excitation spectrum) is not available, huge discrepancies are expected. As a matter of fact, at least for light systems, the main DC contributions to the cross section are generally resulting from transitions to the ground state or to a small number of low-lying states, provided the selection rules authorized the considered electromagnetic transitions. The uncertainties related to the exact determination of the spin and parity of these levels (and to a lower extent, their energy) can modify the DC contribution by many orders of magnitude. The selection rules depend on the exact spin and parity differences between the initial and final states and act as a real switch, turning on or off the direct capture. The smaller the number of contributing levels, the larger the impact of an erroneous spin and parity affectation will be. In a similar way, the energy of the final state can also allow or forbid a transition according to its relative location with respect to the neutron separation energy. The larger the Q-value of the transition, the larger the contribution to the final cross section (see Eq. 2).

As mentioned above, the main contributing levels in the residual nucleus are characterized by a single-particle configuration for which $S_f \simeq 1$. For this reason, most of the previous studies have tried to predict the DC cross section assuming a 1 neutron particle-hole configuration deduced from the single-particle level scheme (e.g. Oberhummer et al., 1995). Unfortunately, this approach lead to large deviations (reaching several orders of magnitude) between the predicted DC cross sections and experimental data, because of the remarkable sensitivity of the cross section to the exact determination of the very few available final states. Moreover, different nuclear structure input lead inevitably to considerable scattered predictions. To avoid such difficulties related to the single-particle approach, we consider here all the possible nucleon excitations, as described by nuclear level density models. In this case, the full single-particle strength is fragmented among the different levels, so that to each of them should be attributed its corresponding spectroscopic factor, or in a first approximation an average spectroscopic factor. The total DC cross section is then expressed as

$$\sigma^{DC}(E) = \sum_{f=0}^{x} C_f^2 \; S_f \; \sigma_f^{DC}(E) + \langle C^2 S \rangle \int_{E_x}^{S_n} \sum_{J_f,\pi_f} \rho(E_f, J_f, \pi_f) \; \sigma_f^{DC}(E) \; dE_f \; , \quad (6)$$

where x corresponds to the last experimentally known level of excitation energy E_x (smaller than the neutron separation energy S_n). Above E_x, the summation is replaced by a continuous integration over the spin (J)- and parity (π)-dependent level density ρ, and the spectroscopic factor and isospin Clebsh-Gordan coefficient by an average quantity $\langle C^2 S \rangle$. Different models of nuclear level densities are now available, although most of them are based on the statistical approach which does not enable a detailed description, especially at low energies, of the spin and parity distributions. Because of the high sensitivity of the DC cross section to these quantities, only the microscopic combinatorial approach seems appropriate. In particular, the combinatorial Monte Carlo technique derived by Cerf (1994) has been shown to be a reliable tool for calculating spin- and parity-dependent level densities with a sufficient accuracy and a short computation time which enable an exact treatment of the BCS pairing and its application to large-scale calculations. This method predicts relatively well the experimental neutron spacing data at the neutron separation energy for spherical nuclei, but tends to underestimate the level density in deformed nuclei, because of its neglect of deformation and collective effects. We consider as standard input for the combinatorial method the realistic ETFSI single-particle level scheme in order to obtain an evaluation of the excitation spectrum as coherent as possible with other ingredients in the calculation (which are all based on ETFSI predictions of nuclear structure properties). Finally, as classically done when dealing with experimentally unknown nuclei, the ground-state spins and parities are determined from ETFSI single-particle configuration applying the simple Nordheim's rule.

So far, the determination of the spectroscopic factor remains an unsolved problem. Closed shell nuclei often have low-lying levels with a high-purity single-particle configuration, but away from magic numbers, or at increasing excitation energy, residual interactions, as well as couplings of the single-particle motion to other degrees of freedom, distribute the spectroscopic strength of a single-particle state among several nuclear levels. Experimental (d,p) reactions clearly show the spreading and fragmentation of the single-particle states which give a continuous spectroscopic strength if the fragmentation width is larger than the spacing of the single-particle states (e.g. Back et al., 1974). In this case, it seems legitimate to approximate the spectroscopic factor by an average value $\langle C^2 S \rangle$. As classically done in nuclear astrophysics (e.g. Caughlan and Fowler, 1988), but without a rigorous physical justification, we adopt $\langle C^2 S \rangle = 0.1$.

Finally, let us note that all the calculations assume a spherical symmetry. Deformations can play an important role in DC mechanism by modifying the single-particle configuration or

[3] Other comparisons of experimental (n, γ) cross-sections with the DC potential model predictions can be found for example in Mengoni et al. (1995) or Oberhummer et al. (1995).

slowing down the process when nucleon reordering is necessary (Rauscher et al., 1995). However, due to the large uncertainties already existing in the spherical approximation of the DC model, as well as the nuclear level density model, it seems presumptuous to treat deformation in detail at the moment. We will neglect deformation effects in the whole nuclear chart. In the same spirit, we only consider $E1$-type transitions which are dominant, if allowed. If no $E1$-transition is possible, $M1$- or $E2$-transitions can then take over, but give rise to much smaller neutron capture rates which are expected to be negligible in comparison with β-decay rates, at least for neutron-rich nuclei. In this respect, there is little significance for r-process applications to determining transitions slower than the $E1$ one.

3. Total neutron capture rates of neutron-rich nuclei

3.1. The radiative DC cross section

All the nuclei potentially involved in the r-process nucleosynthesis, i.e lying in the nuclear chart (with $20 \leq Z \leq 92$) between the valley of β-stability and the neutron-drip line predicted by ETFSI mass model, are considered. The DC contribution is calculated as explained in the previous section, making use of experimental excitation spectrum when available (Eq. 6). Fig. 3 shows the calculated Maxwellian averaged DC rates, $N_a\langle\sigma v\rangle^{DC}$ (where N_a is the Avogadro number, and v the relative velocity between target and projectile) at T_9 = 1.5 (where T_9 denotes the temperature in 10^9 K) for the 3100 neutron-rich nuclei. It is of interest to see that, in contrast to previous calculations (Mathews et al., 1983), the DC rates decrease with decreasing neutron separation energies, as does the CN contribution. This result is to be expected since the number of levels with excitation energy smaller than S_n decreases with decreasing S_n, and with it, the DC cross section. In the present approach, the transitions to low-lying levels are not the only ones to contribute to the total cross section. The high-lying levels have a relatively small contribution to σ^{DC} due to the small k_γ in Eq. 2, but the exponentially rising number of levels with increasing excitation energy compensates this effect in some respect. This is shown in Fig. 4 where the DC rate is plotted as a function of the total number of levels within the $[0, S_n]$ range. The DC rate is clearly proportional to the number of available levels, and therefore does not only depend on transitions to low-lying states. A lower limit of 10^{-5}cm^{3}s^{-1}mol^{-1} imposed on the DC rates (as seen in Figs. 3 and 4) indicates that for some nuclei with low S_n the DC rates can become negligible, the selection rule forbidding the $E1$-type transition to any of the available excited levels. This interesting feature is independent from our adopted value of the average spectroscopic factor and is more significantly illustrated in Fig. 5 where in the (N, Z) plane the half-lives against neutron capture, $\tau_n = 1/N_n\langle\sigma v\rangle^{DC}$, is estimated for a typical neutron density of $N_n = 10^{27}$cm^{-3}. At such a density, many nuclides close to the neutron drip line have a neutron capture half-life longer than 1 ms or even 1 s. In particular, many neutron-rich isotopes of the same element (e.g. Kr, Ba, Yb), show the same hinderance against direct neutron capture.

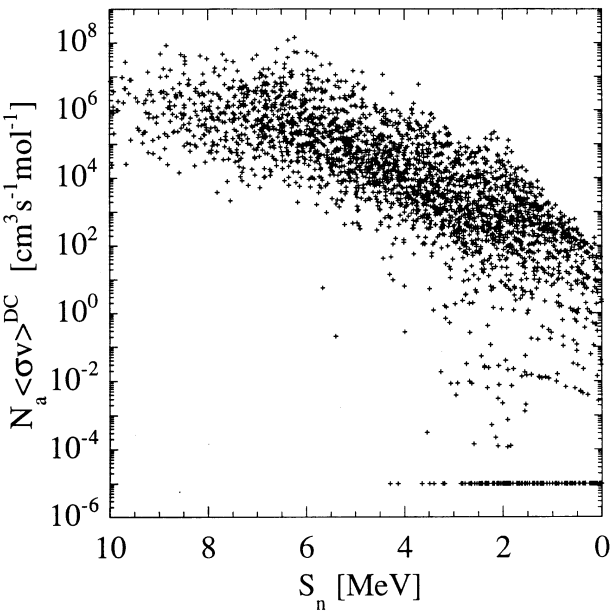

Fig. 3. Variation with S_n of the DC contribution to the Maxwellian-averaged (n, γ) rate calculated for 3100 neutron-rich nuclei at T_9 = 1.5. A lower limit of 10^{-5}cm^{3}s^{-1}mol^{-1} is imposed.

It mainly corresponds to the large decrease of the level density at low energy (due to pairing or shell effects) and to the resulting small number of allowed transitions. Most of them do not fulfill the $E1$ selection rules, because of the appearance of an high-spin state (such as $1i13/2$ in ^{180}Yb). However, it should be noted that level crossings resulting from deformation effects could modify the spin and parity predictions of the low-lying states, and thus transform the forbidden into allowed transitions. A canonical r-process path at T_9 = 1.5 and $N_n = 10^{27}$ cm^{-3} (i.e characterized by the astrophysical parameter S_a^0 = 2.2 MeV–for more details, see Goriely and Arnould, 1992) is also represented in Fig. 5. The implication of these low DC rates on the r-process nucleosynthesis is discussed in Sect. 4.

3.2. Comparison of the DC cross section with the CN contribution

The CN contribution to the (n, γ) rate is calculated within the Hauser-Feschbach model (Thielemann et al., 1986) for which all the nuclear structure properties are taken from the ETFSI model. In particular, the nuclear level density is derived within the microscopic approach of the statistical model based on the same ETFSI single-particle levels as for the DC part (at least for spherical nuclei). It should be noted that the combinatorial is not used in this case, because of its inability at the moment to treat deformed nuclei correctly. The statistical model also presents the advantage of taking into account rotational and vibrational enhancements, as well as the disappearance of deformation at increasing excitation energies. As a consequence the statistical approach shows much closer agreement with experimental data than does the combinatorial model. The complete level density

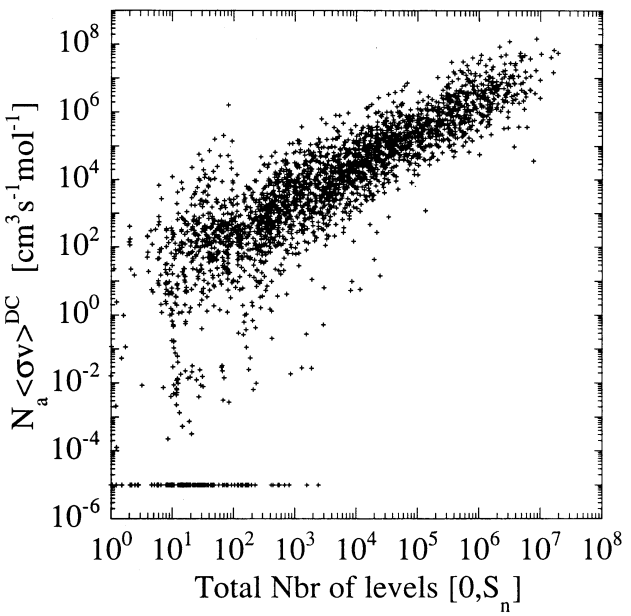

Fig. 4. Same as Fig. 3, but as a function of the total number of levels in the $[0, S_n]$ range.

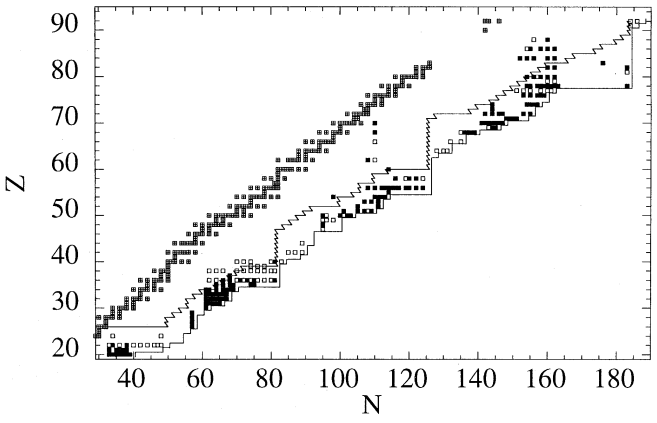

Fig. 5. Representation in the (N, Z) plane of the nuclides with a half-life against neutron DC larger than 1s (full squares) or ranging between 1ms and 1s (open squares) for $N_n = 10^{27}\text{cm}^{-3}$ and $T_9 = 1.5$. The upper left line corresponds to a canonical r-process path in the same thermodynamic conditions. The right line indicates the ETFSI prediction of the neutron drip line. The crossed squares represent the stable isotopes.

prescription adopted here is described in detail in Arnould and Tondeur (1981) and Goriely (1996).

Fig. 6 compares the direct with the statistical contributions to the Maxwellian-averaged radiative capture rate (at $T_9 = 1.5$) for the 3100 neutron-rich nuclei. Close to the valley of stability, the DC rate appears to reach 1 to few tens of percent of the CN prediction. This conclusion is of course bound to our assumption $\langle C^2S\rangle = 0.1$, a lower value leading to a smaller DC contribution. In this case, it contradicts the usual idea that the DC contribution is by far negligible compared with the CN counterpart for heavy stable nuclei. The large DC contribution comes mainly from the high-lying states which lead the DC

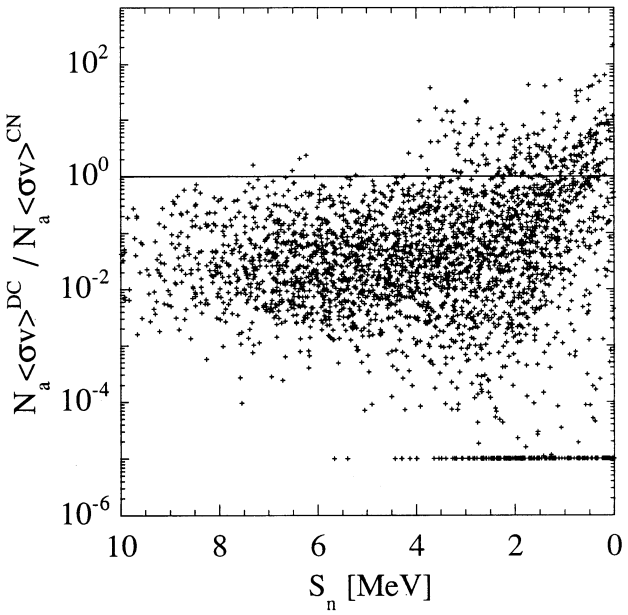

Fig. 6. ratio of the DC to CN contributions to the Maxwellian-averaged (n, γ) rates of the 3100 neutron-rich nuclei at $T_9 = 1.5$.

rate to behave in a similar way as does the CN rate, i.e proportionally to the level density. Of course, many uncertainties related, in particular, to the estimate of the excitation spectrum and the spectroscopic factor, still affect the DC predictions, and further improvements of the microscopic model are required before drawing conclusions on the relative contributions of the DC and CN rates. In particular, the amplitude of the adopted average spectroscopic factor is subject to discussion. In contrast to the nuclei close to the valley of β-stability, the very neutron-rich nuclei present a DC rate with a much more scattered behaviour with respect to the CN rate. For these exotic nuclei, the question of the reliability of the CN model is also bound to arise.

3.3. The total neutron capture cross section

Direct and compound nuclear reactions are known not to be mutually exclusive. Both mechanisms may contribute to the radiative capture of a neutron. For this reason, the total capture rate is often taken as the simple sum of both contributions, neglecting all possible interferences between them. In the popular picture of Mathews et al. (1983), the CN contribution is by far dominant for nuclei close to the valley of stability and decreases rapidly when considering more and more neutron-rich isotopes (especially when crossing a magic neutron number), while the DC remains almost constant; in this case, the transition from the CN regime to the DC one takes place rapidly within an isotopic chain and the total cross section can be relatively well approximated by the sum of both contributions. However, in our present approach, both parts are roughly proportional to the level density in the residual nucleus and decrease similarly as a function of the neutron excess. No fast transition from one regime to another is observed.

Moreover, for nuclei with closed neutron shells or small neutron binding energies, the number of available resonances is very low, so that the statistical model of Hauser-Feschbach cannot be applied. To justify the use of the CN approach, it is usually requested that the available resonance states are "numerous" and that their widths and energies are randomly distributed within the contributing energy interval ΔE. However, no detailed study has been done so far to quantify this high-level-density rule. It should also be reminded that the CN approach always assumes the existence of dominant s-wave resonances, because of the Gaussian spin distribution of the level density inherent to the statistical model. Therefore, we consider here the CN model to be valid if the level density is high enough to ensure that no spurious s-wave resonance is introduced in the excitation spectrum, or quantitatively that the number of levels with the most probable spin in the energy interval ΔE is equal to the arbitrary value of 10. This corresponds to a total nuclear level density at S_n of $\omega^* \simeq 6000$ MeV^{-1} for $\Delta E = 250$ keV. If the total level density at the neutron binding energy is smaller than ω^*, only few CN resonances should be considered in a R-matrix-type calculation, or even in a more simple Breit-Wigner approach. Another possible approach would be the so-called pre-equilibrium process characteristic of high-energy collisions where particles can be emitted after the first direct interaction, and before the statistical equilibrium can be reached. In our case, the non-attainment of the statistical equilibrium is essentially due to the decrease of the number of available resonances. Unfortunately, none of these models have been applied to the determination of the neutron capture cross sections of neutron-rich nuclei. Therefore, we adopt in the present work a more phenomenological approach and estimate the total neutron capture rate by

$$\langle \sigma v \rangle = \langle \sigma v \rangle^{DC} + \langle \sigma v \rangle^{CN} \tag{7}$$

or

$$\langle \sigma v \rangle = \langle \sigma v \rangle^{DC} + \langle \sigma v \rangle^{CN} \; \frac{1}{1 + (\omega^* / \omega(S_n))^{1/a}} \quad , \tag{8}$$

where $\omega(S_n)$ is the total level density at the neutron separation energy and a is a damping parameter characterizing the disappearance of the CN contribution at level densities decreasing below ω^*. Two different values of the damping parameter are considered, namely $a = 0.8$ corresponding to a relatively slow decrease of the CN contribution with $\omega(S_n)$ and $a = 0.2$ describing a faster decrease. These different approximations of the total (n, γ) rates enable us to study the competition between neutron captures and β-decays taking place during the r-process, allowing for an erroneous CN calculation of (n, γ) rates for very exotic nuclei.

4. Influence of the DC on the r-process nucleosynthesis

To understand the possible impact of the DC mechanism on the r-process nucleosynthesis, we consider first the simple canonical model, but without making use of the WPA, i.e without assuming the *a priori* establishment of an $(n, \gamma) - (\gamma, n)$ equilibrium. A full reaction network is solved for a given set of astrophysical parameters (T, N_n, τ_{irr}). Full details of this non-equilibrium canonical model can be found in Goriely and Arnould (1996). The (n, γ) rates are calculated with Eq. 7 (referred to as case I) and Eq. 8 with $a = 0.8$ (case II) or with $a = 0.2$ (case III). Fig. 7 shows the abundance distribution resulting from 1 event ($T_9 = 1.5, N_n = 10^{25}$ cm$^{-3}, \tau_{irr} = 0.8$ s). In this example, the r-process path (characterized by the astrophysical parameter $S_a^0 = 2.8$ MeV) is far enough from the neutron drip line, so that no important effect of the DC contributions is seen in neither of the 3 cases. In each isotopic chain, the produced nuclides have always neutron capture and photodisintegration rates relatively fast compared with the β-decay rates[4]. On the contrary, interesting features can be observed in Fig. 8, when the r-process path gets closer to the drip line ($S_a^0 = 2.2$ MeV). Even at temperatures and neutron densities as high as those considered in Fig. 8–which would have led us to believe in the establishment of the $(n, \gamma) - (\gamma, n)$ equilibrium–the (n, γ) rates are relatively low, especially in case III, and the β-decays can compete with neutron captures for many isotopes along the r-process path. This is well illustrated in Fig. 5, where the canonical path is seen to cross many nuclei with timescales against the neutron DC longer than 1 ms or even 1 s. For many of these nuclei, $\omega(S_n) < \omega^*$, so that the total neutron capture rate is given by the DC component only, and β-decays become dominant with respect to the neutron captures. This non-equilibrium competition is the most effective where the r-process path is the closest to the drip line, i.e. where it reaches the neutron shell closures. Consequently, the final abundance distribution before the main peaks (especially at $A \simeq 115$) is different than the one predicted by the canonical equilibrium model. This feature is similar to the non-equilibrium effect emphasized by Goriely and Arnould (1996) at low neutron densities or temperatures. However, in the present work, it originates from the low neutron capture cross sections, and therefore remains at high temperatures and neutron densities.

A second r-process model, called the multi-event r-process model, is now considered to estimate the impact of the DC. In such a model a given number of different non-equilibrium canonical events are superposed in order to reproduce the solar system r-abundance distribution as precisely as possible. When trying to explain the origin of the solar system r-abundances, this more elaborate model enables us to analyze the impact of nuclear physics uncertainties, such as those related to the estimate of (n, γ) rates, not only on the final abundance distributions, but also on the thermodynamic conditions required to produce the r-elements in solar quantity. More details, and in particular the fitting procedure, can be found in Bouquelle et al. (1996) and Goriely and Arnould (1996). Fig. 9 compares the normalized solar system r-abundances with those obtained from the best-fit superposition of the multi-event r-process restricted to the thermodynamic conditions, $1 \leq T_9 \leq 2$ (grid steps of 0.2), $10^{20} \leq N_n(\text{cm}^{-3}) \leq 10^{27}$ (grid steps of 10) and

[4] Note that the β-decay half-lives are estimated by the revised version of the gross theory (Tachibana et al., 1990).

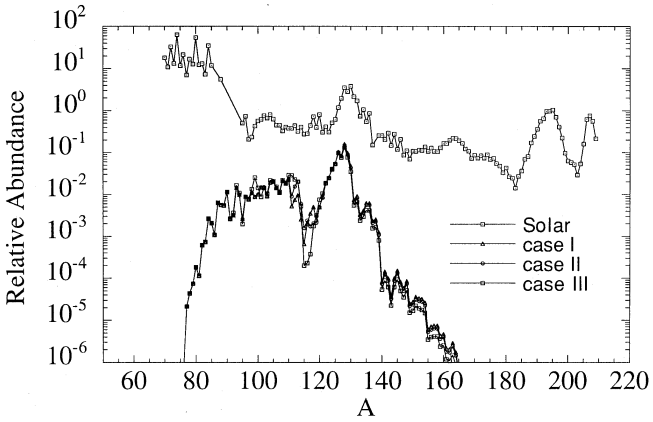

Fig. 7. r-process yield curves obtained in the framework of the non-equilibrium canonical model for the set of physical parameters T_9 = 1.5, $N_n = 10^{25}$ cm^{-3} and τ_{irr} = 0.8 s. The 3 curves are obtained for the 3 different estimates of the total (n,γ) rates (see text). The top curve corresponds to the r-process abundances (Anders et Grevesse, 1989) arbitrarily normalized.

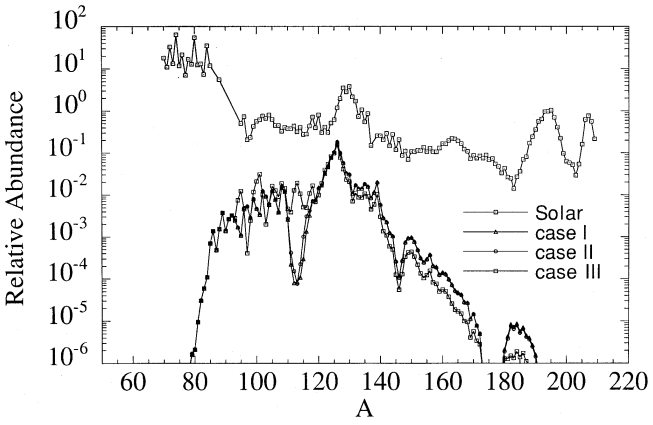

Fig. 8. Same as Fig. 7, but for T_9 = 1.5, $N_n = 10^{27}$ cm^{-3} and τ_{irr} = 0.4 s.

$10 \leq n_{cap} \leq 150$ (grid steps of 7.5)[5]. Maximum irradiation times of τ_{max} = 3 s are considered. The multi-event r-process is calculated for cases I to III. They all appear to give a relatively good fit to the solar system abundances, no significant discrepancies being observed. The normalized statistical weights of the events involved in the fits of Fig. 9 are displayed in Figs. 10, 11 and 12 for cases I, II and III, respectively. As seen in Figs. 9-12, the changes in the nuclear physics considered do not affect the abundance distributions anymore, but rather the statistical distributions of the events involved. Because of a possible contribution of the α process in the production of the $70 \leq A \leq 100$ nuclei (Takahashi et al., 1994; Woosley et al., 1994), our results in this mass region are of no significance without a prior study of the α-process nucleosynthesis. On the one hand, the main $A \simeq 130$ and $A \simeq 195$ peaks appear to be explained in the three cases by similar events, characterized by r-process paths in the 2 MeV $\leq S_a^0 \leq$ 3 MeV range. On the other hand,

[5] n_{cap} is the number of neutrons captured by the seed nuclei of ^{56}Fe.

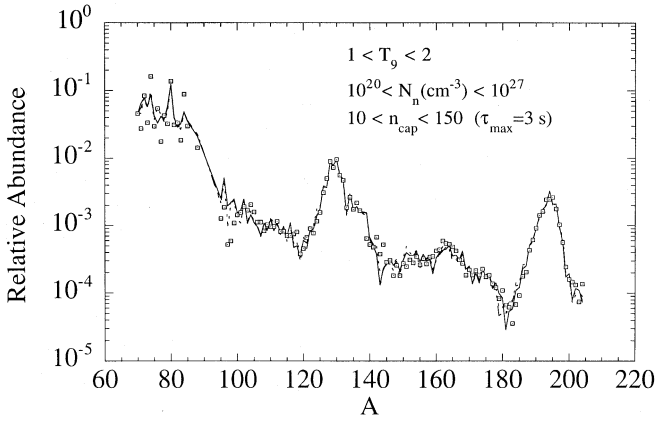

Fig. 9. Fit to the solar system r-abundances derived from a superposition of non-equilibrium canonical events. The grids of considered values of T_9, N_n and n_{cap} are given in the main text. Cases I, II and III are represented by full, dot-dash and dotted line, respectively. They all give a similar fit to the solar distribution.

differences can be observed in the events responsible for the production of the $A \simeq 115$ and $A \simeq 140$ elements. In particular, the fit to the pre-peak $A \simeq 115$ nuclei call for events at low S_a^0 values in case I, while these events are not required anymore in case III. As already shown by Goriely and Arnould (1996), the production of the $A \simeq 115$ nuclei can be explained by considering non-equilibrium (i.e low-temperatures or low-neutron-densities) events or low-S_a^0-value (i.e low-temperatures and high-neutron-densities) events. In case III, the slow neutron captures lead to the same effects as the low-temperatures, low-densities effects and enable the production of the pre-peak nuclei by astrophysical events with $S_a^0 \simeq 2.7$ MeV and $T_9 \simeq 1.3-1.5$, i.e the same as the one responsible for the A = 130 peak elements. In case I, such events are not effective to produce the pre-peak elements, and high-density events with $S_a^0 \simeq 1.6$ MeV play an important role. In case III, these low-S_a^0 events appear to be more efficient in the production of the $A \simeq 140-150$ nuclei, as seen in Fig. 11. Note that in the intermediate case II, none of the low-S_a^0 r-processes contributes significantly anymore; the bulk solar system r-abundances are produced by events with 2 MeV $\leq S_a^0 \leq$ 3 MeV only, and in particular the synthesis of $A \simeq 115$ nuclides requires events characterized by low temperatures $T_9 \simeq 1-1.1$ and low neutron densities ($N_n \simeq 10^{23}$cm^{-3}). The production of the $A > 150$ r-elements in solar abundances calls for globally the same events in cases I, II and III.

Finally, it is of interest to investigate the influence of the newly-derived (n,γ) rates on the validity of the WPA. To do so, we consider the same criteria as defined by Goriely and Arnould (1996), i.e. the deviation between the final abundances of a given canonical event (CE) obtained with the WPA (N(CE)) and without the WPA (N(NECE), where NECE stands for non-equilibrium canonical event). This deviation is expressed by the root mean square factor

$$f_{rms} = \exp\left[\frac{1}{n_{tot}}\sum_{i=1}^{n_{tot}} \ln^2 \frac{N_i(\mathrm{CE})}{N_i(\mathrm{NECE})}\right]^{1/2}, \quad (9)$$

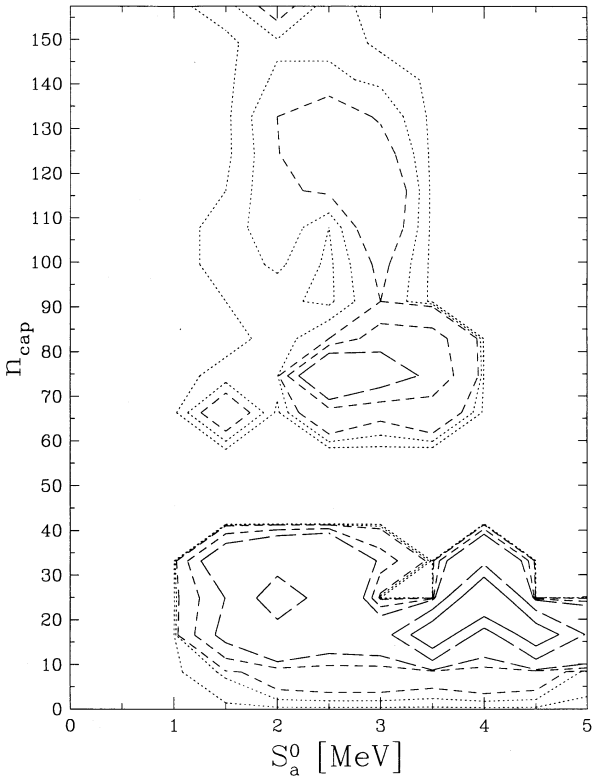

Fig. 10. Representation in the (S_a^0, n_{cap}) plane of the statistical weights of the events involved in the abundance fit of Fig. 9 for case I. The contours of normalized values of 10^{-4} and 5 10^{-4} are shown by dotted lines. The contours of 10, 100 and 1000 times larger values are represented by short dashed, long dashed and solid lines, respectively.

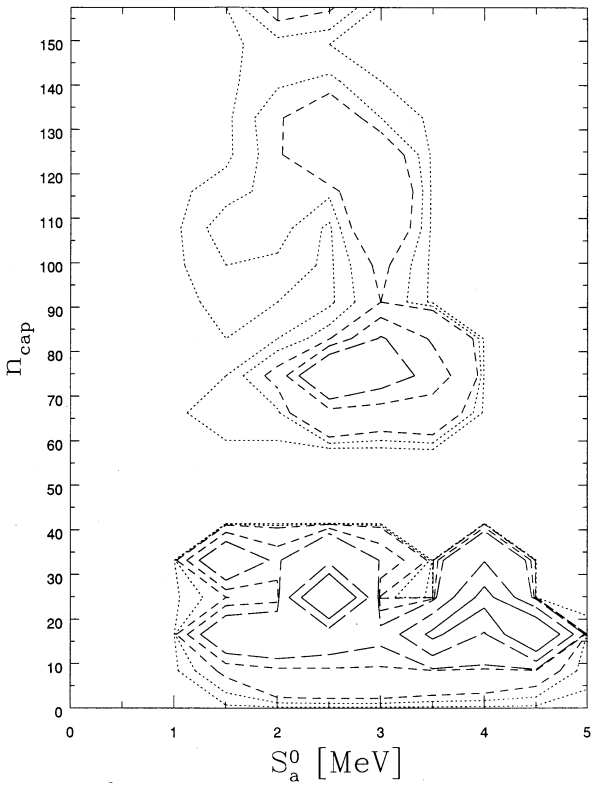

Fig. 11. Same as Fig. 10, but for case II.

where i runs over the n_{tot} nuclidic species i. The f_{rms} factor are calculated for some 3000 events in the ranges $1 \leq T_9 \leq 2$, $10^{20} \leq N_n(\mathrm{cm}^{-3}) \leq 10^{30}$ and $10 \leq n_{cap} \leq 150$. Since f_{rms} does not depend drastically upon n_{cap}, it is profitable to define an average $\langle f_{rms} \rangle$ factor for each (T_9, N_n) couple. The $\langle f_{rms} \rangle$ factor provides then a direct and quantitative evaluation of the validity of the WPA. For $\langle f_{rms} \rangle \lesssim 2$, the WPA can be considered as a good approximation, while large errors can be expected if use is made of the WPA for astrophysical conditions such that $\langle f_{rms} \rangle > 2$. Fig. 13 displays the equi-$\langle f_{rms} \rangle$ lines in the (T_9, N_n)-plane calculated with the (n, γ) rates taken from case I and case III. In case I, the WPA remains valid in a relatively similar region of the (T_9, N_n)-plane as described by Goriely and Arnould (1996), since the total (n, γ) rate is essentially given by the CN part. On the contrary, in case III, the validity of the WPA appears to be shifted to much higher N_n and T_9 values, because of the much smaller CN contribution considered for very neutron-rich nuclei. In particular, at temperatures $T_9 \leq 1.5$, the $(n, \gamma) - (\gamma, n)$ equilibrium is never reached, since these events are characterized by r-process paths close to the neutron-drip line, where small neutron capture cross sections are encountered. Of course, it should be added that all our conclusions are affected by the remaining uncertainties in the prediction of the β-decay rates for very exotic nuclei. The situation will hopefully be improved by the new calculations to come in the semi-gross theory approach (Nakata et al., 1997), as well as in the self-consistent microscopic model of finite Fermi systems (Borzov et al., 1996).

5. Conclusions

The neutron capture reactions play a pivotal role in the r-process nucleosynthesis. Unfortunately, the difficult task to estimate the (n, γ) rates for the numerous neutron-rich nuclei involved in the r-process is quite often avoided by calling for simplified assumptions, such as the WPA. However, even the WPA is bound to a reliable estimate of the neutron capture rates to justify its applicability. Therefore, a reliable prediction of the neutron capture rates is mandatory. We have tried to estimate the DC, as well as the CN contributions to the radiative capture of neutrons. In particular, the DC rates are calculated within a microscopic model based on the same potential as the one considered in the CN model. The excited level spectrum in the residual nucleus is predicted by a combinatorial model of nuclear level densities, and the resulting single-particle configuration is assumed to be characterized by an average spectroscopic factor. In this approach, the DC rates are found to be proportional to the number of levels of energy lower than the neutron binding energy. Consequently, the DC mechanism is often not negligible compared with the CN process for nuclei close to the valley of stability. Neutron-rich nuclei present DC rates which show large variations according to the allowed or forbidden $E1$-transitions available between

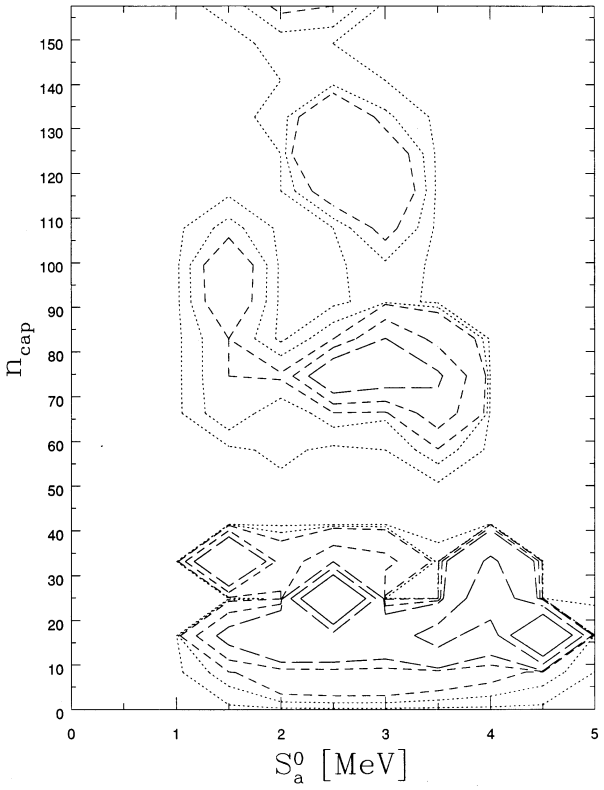

Fig. 12. Same as Fig. 10, but for case III.

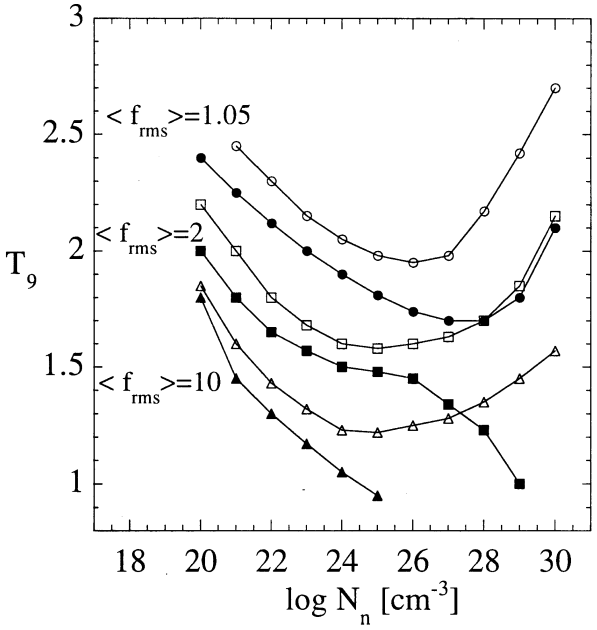

Fig. 13. Limits of validity of the WPA in the (T_9, N_n) plane based on the consideration of about 3000 r-process events. The events corresponding to the values of 1.05 (circles), 2 (squares) and 10 (triangles) of the average deviation factor $\langle f_{rms} \rangle$ are connected with solid lines. The full symbols are obtained with the (n, γ) rates given by case I and the open symbols by case III.

the initial and final systems. Of course, large uncertainties still affect the DC predictions, but our results emphasize the possibility of a negligible DC rate for many neutron-rich nuclei. This might have an important impact on the r-process nucleosynthesis.

The validity of the adopted Hauser-Feshbach model to calculate the CN rate has also to be questioned when dealing with neutron-rich nuclei for which the number of levels at the neutron binding energy might be too low to justify the statistical approach. A phenomenological approximation to the total neutron capture rate is prescribed considering the possibility of a large overestimate of the CN contribution for nuclei with a low level density at the neutron binding energy. In this case, it is shown that the $(n, \gamma) - (\gamma, n)$ equilibrium usually assumed in parametric r-process models might not be fulfilled, even at high neutron densities. A full reaction network has to be solved to allow for the competition between β-decays, neutron captures and photodisintegrations. R-process calculations in the framework of the single-event model indicate that the low (n, γ) rates can affect the r-process paths, mainly where it gets close to the neutron drip line, i.e before the N = 82, and to a lower extent N = 126, shell closures. The final r-abundance distribution is consequently modified before the abundance peaks. Multi-event r-process calculations show that weak neutron captures influence also the thermodynamic conditions of the astrophysical events called to explain the origin of the solar system r-content. In particular, the role of r-process events leading to the production of nuclei close to the neutron drip line is modified according to the total (n, γ) rates adopted. Finally, the validity of the WPA is investigated using the newly-derived (n, γ) rates. It is shown that at temperatures $T_9 \leq 1.5$, the $(n, \gamma) - (\gamma, n)$ equilibrium might never be reached.

The prediction of the DC and CN contributions to the neutron capture rates obviously requires further improvements before drawing conclusions on the effective impact of the neutron captures on the r-process nucleosynthesis. We acknowledge the large uncertainties inherent to the DC model, as well as the CN model to estimate reliably the nuclear reaction rates for experimentally unknown neutron-rich nuclei. In particular, the adopted DC model still suffers from large uncertainties stemming from the predicted excitation spectrum of the residual nucleus. This includes the energy, spin, parity and spectroscopic factors of all the levels below the neutron binding energy. A full knowledge of these quantities are required to improve the predictive power of the DC model. The important effect of nuclear deformation has been neglected here, and should be taken into account. Therefore, it appears, that our understanding of the r-process nucleosynthesis requires an extended knowledge of not only many nuclear structure properties (masses, deformations, shell and pairing effects, nuclear level densities, . . .), but also interaction properties (neutron capture rates, β-decay rates, . . .). Much remains to be done experimentally and theoretically.

Acknowledgements. The author is grateful to P. Descouvemont, N. Cerf, N. Tymofeuk and M. Arnould for very useful discussions. S. Goriely is F.N.R.S. Senior Research Assistant.

References

Aboussir Y., Pearson J.M., Dutta A.K., Tondeur F., 1992, Nucl. Phys. A549, 155
Anders E., Grevesse N., 1989, Geochim. Cosmochim. Acta 53, 197
Arnould M., Tondeur F., 1981, In: Proc. 4th Conf. on nuclei far from stability, Helsingør, CERN 81-09, vol. 1, p.229
Back B.B., Bang J, Björnholm S., Hattula J., Kleinheinz P., Lien J.R., 1974, Nucl. Phys. A222, 377
Baye D., Descouvemont P, 1985, Ann. Phys. 165, 115
Beer H., Coceva C., Sedyshev P.V., Popov Y.P., Herndl H., Hofinger R., Mohr P., Oberhummer H., 1996, Phys. Rev. C to be published
Borzov I.N., Fayans S.A., Krömer E., Zawischa D., 1996, Zeit. Phyz. A 355, 117
Bouquelle V., Cerf N., Arnould M., Tachibana T., Goriely S., 1996, A&A 305, 1005
Caughlan G.R., Fowler W.A., 1988 ADNDT 40, 283
Cerf N., 1994, Phys. Rev. C49, 852; Phys. Rev. C 50, 836
Goriely S., Arnould M., 1992, A&A 262, 73
Goriely S., Arnould M., 1996, A&A 312, 327
Goriely S., 1996, Nucl. Phys. A605, 28
Jeukenne L.-P., Lejeune A., Mahaux C., 1977, Phys. Rev. C16, 80
Kobos A.M., Brown B.A., Lindsay R., Satchler G.R., 1984, Nucl. Phys. A425, 205
Krausmann E., Balogh W., Oberhummer H., Rauscher T., Kratz K.-L., Ziegert W., 1996, Phys. Rev. C53, 469
Lane A.M., Lynn J.E., 1960, Nucl. Phys. 17, 563; 1960, 17, 686
Lynn J.E., 1968, The theory of neutron resonance reactions (Clarendon press, Oxford)
Mathews G.J., Mengoni A., Thielemann F.-K., Fowler, W.A., 1983, ApJ 270, 740
Mengoni A., Otsuka T., Ishihara M., 1995, Phys. Rev. C52, R2334
Nakata H.; Tachibana, T., Yamada M., 1997, preprint
Oberhummer H., Balogh W., Bieber R., Herndl H., Langer U., Rauscher T., Beer H., 1995 In: de Saint Simon M., Sorlin O. (eds) International Conference on Exotic Nuclei and Atomic Masses. Editions Frontières, Gif-sur-Yvette, p. 649
Rauscher T., Böhmer W., Kratz K.-L., Balogh W., Oberhummer H., 1995 In: de Saint Simon M., Sorlin O. (eds) International Conference on Exotic Nuclei and Atomic Masses. Editions Frontières, Gif-sur-Yvette, p. 683
Satchler G.R., 1980, Introduction to nuclear reactions (Macmillan press ltd)
Satchler G.R., 1983, Direct nuclear reactions (Clarendon press, Oxford)
Seeger P.A., Fowler W.A., Clayton D.D., 1965, ApJS 11, 121
Tachibana T., Yamada M., Yoshida Y., 1990, Progr. Theor. Phys. 84, 641
Takahashi, K., Witti, J., Janka, H.-Th., 1994, A&A 286, 857
Thielemann F.-K., Arnould M., Truran J.W., 1986, In: Vangioni-Flam E., Audouze J., Cassé M., Chièze J.-P., Tran Thanh Van J. (eds.) Advances in Nuclear Astrophysics. Editions Frontières, Gif-sur-Yvette, p. 525
Uozumi Y., Iwamoto O., Widodo S., Nohtomi A., Sakae T., Matoba M., Nakano M., Maki T., Koori N., 1994, Nucl. Phys. A576, 123
Wilmore D., Hodgson P.E., 1964, Nucl. Phys. A55, 673
Woosley S.E., Wilson J.R., Mathews G.J., Hoffman R.D., Meyer B.S., 1994, ApJ 433, 229

This article was processed by the author using Springer-Verlag LaTeX A&A style file *L-AA* version 3.